LA-DC - 9989

L. Merrill

PREPRINT FROM

# LOS ALAMOS SCIENTIFIC LABORATORY
## of the
## University of California
### LOS ALAMOS • NEW MEXICO

THE HUGONIOT EQUATION OF STATE OF SODIUM CHLORIDE IN THE SODIUM
CHLORIDE STRUCTURE

By

J. N. Fritz, S. P. Marsh, W. J. Carter, and R. G. McQueen

# The Hugoniot Equation of State of Sodium Chloride in the Sodium Chloride Structure*

J. N. Fritz, S. P. Marsh, W. J. Carter, R. G. McQueen
University of California, Los Alamos Scientific Laboratory

## ABSTRACT

The Hugoniot equation of state of NaCl has been obtained by measuring the shock velocity through NaCl on copper and 2024 aluminum base plates. Shock velocities through the base plates and standard impedance-matching were used to obtain the Hugoniot curves for both single crystal (in various orientations) and pressed powder samples. The smooth behavior of the resulting shock locus up to 230 kb indicates that NaCl exists in the sodium chloride structure up to this pressure. In the shock-particle velocity plane the best linear fit to the data reported here is $u_s$ (km/sec) $= (3.528 \pm .012) + (1.343 \pm .009) u_p$. A quadratic fit, which gives a large weight to the measured bulk sound speed in NaCl, is $u_s = 3.403 + 1.5422 u_p - 0.07345 u_p^2$. Isotherms at $293^O$ K, using different forms for the Grüneisen parameter and a simple Debye model for the specific heat, are calculated from the Hugoniots and are presented here. They should prove useful when NaCl is used as an internal standard in high pressure X-ray devices.

## Introduction

Since Jamieson[1] first used NaCl as an internal pressure standard in his high pressure X-ray apparatus, it has been a serious candidate for a pressure standard in high pressure X-ray work. Decker[2] has advocated the use of NaCl as a standard. His proposal was based on a Born-Mayer equation of state. Parameters were fixed by the initial density and sound speed of NaCl at zero pressure and he achieved a prediction of the curvature of the P-V isotherm, which can be converted in terms of variables familiar to workers in the dynamic-pressure field to a prediction of the slope of the shock velocity vs. particle velocity Hugoniot. His results were supported by the then existing shock wave data. An increase of 1.3 percent in the value of the sound speed he used in his work would bring his isotherm into agreement with the result of the present report.

Objections have been raised[3,4,5] to using NaCl as a standard because of the possibility of the transition to the CsCl structure at a pressure as low as 20 kb. Such a low pressure transition would unacceptably complicate the use of NaCl as a continuous pressure standard. Others[6,7,8,9] have found no evidence for a transition as low in pressure as this. From the work of Jamieson[9,10] on the solution salts, $Na_x K_{1-x} Cl$, one can conclude that the B1 to B2 transition must be considerably above 130 kb in the pure end number,

NaCl. Finally, Bassett et al.[11] have found and reversed the B1 to B2 transition in NaCl at approximately 300 kb at room temperature. It would seem that whatever the remaining phenomena is at 20 kb, it does not involve the B1 to B2 transition, and that NaCl will remain in the B1 structure to high and useful pressures.

Perez-Albuerne and Drickamer[8] have compared NaCl by X-ray techniques with Ag and Mo. If the compression curves of Ag and Mo are known, this would determine a NaCl isotherm. Using older shock wave data[12], results were obtained which, because of the individual scatter in a data point, were used only to verify the calculation of an isotherm from a particular form of a Born-Mayer treatment. Their calculated isotherm is in agreement with the isotherm we report as well as that of Bridgman[6].

Direct shock-particle velocity data on NaCl could not be obtained because of the impracticality of fabricating the assemblies required for our shock-wave techniques. Hence we have employed the shock-wave impedance match technique using 2024 aluminum base plates as the standard. In this way, NaCl becomes a secondary standard, dependent on the Hugoniot and extended equation of state of 2024 aluminum. If the 2024 aluminum Hugoniot is accepted as known, a shock-locus for NaCl is obtained that is felt to be accurate to 1% in pressure. Subsequent modifications, if any, of the primary standard may be easily translated to a new Hugoniot locus for NaCl. As always, the largest uncertainty in an isothermal curve derived from shock-wave data is related to the choice of the

Grüneisen gamma used to reduce the Hugoniot to an isotherm. .
Several functions of volume have been used for $\gamma(V)$ and the
resultant isotherms reported.

## Experimental Methods and Results

The impedance matching technique used for obtaining the
shock locus for NaCl has already been adequately described[12].
Single crystals in the (100), (110) and (111) orientations as well as
some pressed powder samples were shock-loaded on base plates of
2024 aluminum, copper, and 921-T aluminum. The data taken on
921-T aluminum base plates has been discarded for reasons described
elsewhere[13]. In this report only those data whose final shocked
state is believed to remain in the B1 structure are reported. The
majority of the data were taken on 2024 aluminum with a few points
taken on copper base plates as a consistency check. The data
necessary for impedance calculations for the primary standards are:

2024 aluminum:     $\rho_0 = 2.785 \text{ g/cm}^3$, $u_s = 5.328 + 1.338 \, u_p \text{ km/sec}$

$(\partial E/\partial P)_V = 0.19 \text{ cm}^3/\text{gm}$

Copper:     $\rho_0 = 8.93 \text{ g/cm}^3$, $u_s = 3.940 + 1.489 \, u_p \text{ km/sec}$

$(\partial E/\partial P)_V = 0.057 \text{ cm}^3/\text{gm}$.

A constant $(\partial E/\partial P)_V$ was used to generate the release isentropes
necessary for the impedance match calculations. The data are
reported in Table I and illustrated in Fig. 1. In addition to the
tabulated data, data points showing the onset of the B1 to B2
(presumably) phase transition are included in the figure for both

(100) and (111) orientations.

Both linear and quadratic terms in $u_p$ were used to fit these data. In the absence of other information, there would be no point in going to an order higher than linear to fit the data; however, consideration must be given to the measured sound speeds in NaCl. In fact, the $c_0$ coefficient in our quadratic fit was forced to agree with the sound speed obtained from Haussuhl's[14] measurement of the elastic constants of single crystal NaCl. The least squares analysis of the data gives r. m. s. deviation of $\Delta u_s = \pm 0.056$ km/sec or less over the range of the data. Within the range of the data, the quadratic and linear fits agree to within this $\Delta u_s$ except for the lowest four data points. The low shock pressures for these four points (< 40 kb) were produced by relatively complicated driver arrangements that depend on impedance mismatches. It is not impossible that overtaking waves could influence these measurements. The shock velocities at these pressures are notably below some of the single crystal longitudinal velocities. Premature closure of flash gaps could give rise to the sort of discrepancy we see here, but since a low-pressure cannon shot has indicated that the Hugoniot elastic limit of NaCl is only about 2/3 of a kilobar, there is not sufficient motion imparted to a shim to close any flash gaps used here. Gap closure corrections are more critical in this pressure regime and conceivably could cause errors in shock wave velocity, but not of the size to explain these low pressure shots. In any event, forcing the Hugoniot through

the sound speed prevents these points from appreciably influencing
the fit to the data. The large bulk of the data at higher pressure
with its linearity fixes the next two terms of the series. Some
evidence that these lower points influence the slope in the right
direction is afforded by Bartels and Schuele's[15] measurement of
$(\partial B_S/\partial P)_T = 5.27$.

From the thermodynamic identities

$$s_0 = [1 + (\partial B_S/\partial P)_S]/4$$

and

$$(\partial B_S/\partial P)_S = (\partial B_S/\partial P)_T + \gamma (T/B_S) (\partial B_S/\partial T)_P$$

and Haussuhl's[14] value for $(\partial B_S/\partial T)_P$ of $-0.000117$ Mb/$^\circ$K, we
obtain $s_0 = 1.513$. This is in satisfactory agreement with our fitted
slope of 1.542. Although a linear fit represents the shock-wave data
adequately, emphasis should be placed on the ultrasonic measurements
in the low pressure region. The quadratic fit

$$u_s = 3.403 + 1.5422 u_p - 0.07345 u_p^2 \text{ (km/sec)} \tag{1}$$

represents the ultrasonic data in the low pressure region and the
shock-wave data in the high pressure region. The number of significant
figures quoted in the above equation gives the exact form of the Hugoniot
used in a subsequent reduction to an isotherm. The r.m.s. spread in
$u_s$ about the fitted values is $\pm 0.05$ km/sec. Our data for NaCl in the
B1 phase are in agreement with the data of Larson, et. al[3], to within
the quoted error. Unpublished data of Hauver and Melani[16] are in

agreement with ours in the vicinity of $u_p$ = 1 km/sec and are

0.07 km/sec higher than ours near $u_p$ = 2 km/sec. However, their

data were based on the old 2024 aluminum standard. Revision of the

necessary impedance match calculations will bring the results into

better agreement.

## Reduction of the Hugoniot to a 293 $^O$K Isotherm

Details of this calculation have been discussed earlier.[13] The

auxiliary information needed for this reduction is given in Table II.

Original references should be consulted for the accuracy of these

numbers. The table gives the exact input used in our calculations.

The particular numerical code used integrates the equation

$$dT_H = -T_H \frac{\gamma dV}{V} + \frac{\left(V_0 - V\right)dP_H + P_H \, dV}{2 \, C_V} \tag{2}$$

for the temperature along the Hugoniot. A Debye expression,

$$E_T = 3nkT \, D_3 \left(\theta \, (V)/T\right) \tag{3}$$

$$D_3(x) = \frac{3}{x^2} \int_0^x \frac{z^3 \, dz}{e^z - 1} \tag{4}$$

$$\gamma = -d \ln \theta / d \ln V \tag{5}$$

is used for the thermal part of the energy.

With a $\gamma$ that depends only on volume, the appropriate fractional

thermal energy and corresponding thermal pressure may be subtracted

from the Hugoniot to yield the desired isotherm. The choice of Debye

is a generalization of the Slater, Dugdale - MacDonald and Free

Volume relations between $\gamma(V)$ and $P_K(V)$ which has been used by

Grover et. al.[22] in their comparison of static and dynamic high-

pressure data on the alkali metals. Values of t of 0, 1 and 2

correspond to the above theories, but the value of t can be chosen

to give the proper thermodynamic value of $\gamma$ at the Hugoniot centering

point. Further, if the expression for $\gamma(V)$ obtained from differences

between the Hugoniot curve and the zero Kelvin curve is equated

with the above expression for $\gamma$, the Hugoniot centering point is

taken to be at zero pressure and temperature, and a linear $u_s - u_p$

Hugoniot is used, an integro-differential equation for $P_K(V)$ is

obtained. When solved this gives not only $P_K(V)$, but also a $\gamma(\eta)$,

where $\eta = 1 - \rho_0 V$, that parametrically depends only on t and the

slope, s, of the $u_s - u_p$ Hugoniot. At zero compression, this reduces

to the relation

$$\gamma_0 = 2s - (t + 2)/3 \tag{7}$$

between $\gamma_0$, t, and s. A linear $u_s - u_p$ Hugoniot for NaCl that passes

through most of the shock wave data and the measured sound speed

has s = 1.429. With the correct $\gamma_0$, (7) yields t = 1.761. The

$\gamma(\eta)$ obtained in this fashion will not significantly differ from one

where the precise experimental Hugoniot is used as input and where

the difference between the temperature of the Hugoniot centering

point and zero temperature is taken into account. The resulting $\gamma(\eta)$,

as well as others, are shown in Fig. 2. This $\gamma(\eta)$ may be accurately represented by a polynominal in $\eta$ for $0 < \eta < 0.5$.

$$\gamma = 1.6044 - 0.9955\eta + 1.4961\eta^2 - 1.9284\eta^3 \qquad (8)$$

This representation, along with the more precise Hugoniot fit, was then used in the numerical code that calculates the isotherm. The resultant curve, labelled (1), is shown in Fig. 3. An ionic solid may not be the best place to use such a theory for $\gamma(\eta)$, but it does offer an alternate $\gamma(\eta)$ behavior to compare with the base isotherm.

Another $\gamma(\eta)$ behavior is offered by Decker[2]. A term linear in the change in lattice parameter was added to $\gamma_0$ to give the best fit to high temperature (i.e., a slight increase in volume) thermal expansion data. This should give the right initial slope of $\gamma(\eta)$ but as Decker says, it is uncertain whether this volume dependence remains accurate to the large volume changes obtained in the shock wave data. This $\gamma(\eta)$ is given by

$$\gamma = 1.6044 + 2.55((1-\eta)^{1/3} - 1) \qquad (9)$$

Decker actually used the value $\gamma_0 = 1.59$. A polynominal fit to (9) was used to calculate isotherm (2) in Fig. 3.

Isotherms (3) and (4) show the effect of varying $\gamma_0$ by plus and minus 10%. For these isotherms $(\partial E/\partial P)_V$ was kept constant. Isotherms (5) and (6) show the effect of scaling $C_v$ by plus and minus 10%. This was done by changing the value of 3nk in the calculations. Isotherms (7) and (8) were obtained by adding and subtracting, respectively, 0.05 km/sec to $c_0$ in the input Hugoniot.

## Comparison with other Isothermal Data and Discussion.

The "base isotherm" is shown in Fig. 4 along with Decker's,
that calculated by Perez-Albuerne and Drickamer, and Bridgman's
data. The agreement between our isotherm and that of Perez-Albuerne
and Drickamer's is well within the experimental error of both methods.
The latter isotherm is slightly lower (1-2 kb) than ours in the pressure
range from 40 to 100 kb. Bridgman's isotherm is still lower by again this
pressure difference in this region. The lower portion of our isotherm
is chiefly determined by using Haussühl's sound speed. The initial
slope of the $u_s$-$u_p$ Hugoniot could be changed from 1.542 to 1.512 to
agree with Bartels and Schuele, but this would decrease the computed
isotherm by only 1/4 kb at 40 kb. At 60 kb, the shock-wave measure-
ments are slightly above the fit used. Above this, where the shock
wave measurements should be relatively free of elastic-plastic flow
effects because of the low Hugoniot elastic limit of NaCl, the fit and
the data are consistent. Decker's isotherm falls below ours, with the
spread in pressure being about 5 kb at 100 kb, 12 kb at 200 kb, and
remaining approximately the same thereafter. As he noted, Decker's
isotherm is most sensitive to the value of the bulk modulus used. A
choice of bulk modulus equivalent to the sound speed we have used
would bring the two isotherms into essential agreement. It is perhaps
worthwhile to emphasize at this point that at and above 80 kb, and to
a lesser extent at 60 kb, our isotherm does not particularly depend on

on the precise value of the bulk modulus used, because the shock-
wave data then determines the Hugoniot used to calculate the isotherms.

Jeffrey, et. al.[23] have given the pressures of various phase
transitions by determining $a/a_0$ of NaCl used as an internal standard.
Using their values of $a/a_0$ and Decker's pressure scale they obtain
$24.8 \pm 0.8$ kb for the Bi I-II transition, $53.3 \pm 1.2$ kb for the Ba I-II
transition, and $73.8 \pm 1.3$ kb for the Bi III-V transition. Using our
isotherm and their $a/a_0$ values these numbers become $25.8 \pm .8$,
$56.3 \pm 1.2$ and $78.2 \pm 1.3$. Bridgman's volume scale as reported
by Jeffrey, et al., has 25.4, 58.8 and 88 kb for these transitions,
McWhan[24] also measured the Bi III-V transition with NaCl as an
internal standard. He took his values on the increasing pressure
cycle, whereas Jeffrey, et. al, averaged increasing and decreasing
pressure readings. McWhan's $V/V_0 = 0.816 \pm .006$ corresponds to
$81.7 \pm 4.5$ kb on our isotherm. The Birch-Murnaghan equation and
the input parameters as used by McWhan for his pressure value is
consistent with our isotherm up to a pressure of 100 kb. Beyond that,
the Birch-Murnaghan value for the pressure increases more rapidly
than our isotherm by 6 kb at 150 kb and 13 kb at 200 kb.

The highest measured pressure on our Hugoniot for the B1
phase is 264 kb. The offset down to the isotherm is about 16 kb at
this volume. Our isotherm above 250 kb is then a consequence of an
extrapolation of the Hugoniot data. The downward curvature of the
quadratic $u_s$-$u_p$ fit is a relic of trying to fit the ultrasonic data and

shock data smoothly together in the lower pressure region and probably should not be there. Both the data alone and calculations of a $u_s$-$u_p$ curve from a Born-Mayer form for the interaction potential indicate a linear behavior in this region. Accordingly we have listed in Table IV the isotherm above 200 kb that obtains from the best linear fit to our data. In this calculation we have again used constant $(\partial E/\partial P)_V$. From 200 to 230 kb this is essentially identical to the isotherm resulting from the quadratic fit. Above 230 kb it becomes stiffer.

A clear indication of a phase transition is exhibited by the higher pressure data points plotted in Fig. 1. Although (111) and (100) oriented crystals have indistinguishable Hugoniots at lower pressures, they clearly separate in the region where the phase transition occurs. Since a uniaxial compression of 50% in the (111) direction produces the B2 structure from the B1 structure, one can expect that a shock wave in this direction will see a lower energy barrier in the way of this transition. Indeed, the (111) data are lower. If a shock wave is not complicated by relaxation effects and deviatoric stresses, a phase transition with a sufficient $\Delta V$ and an appropriate slope in the P-T plane appears as a horizontal plateau in the $u_s$-$u_p$ plane. This is because the flash gaps measure the shock velocity of the first wave in a two-wave structure, which remains constant as we increase the driving pressure, and the particle velocity, measured indirectly by measuring the shock velocity of the standard, is increasing with the

driving pressure. Time dependent effects clearly influence the
NaCl data in this region, but the onset of a phase transition is
beyond question. At these pressures, even though a considerable
time may be required for a phase transition to go to completion,
any part of the $\Delta V$ of the reaction manifests itself immediately as
a shock velocity less than would be expected from a smooth continuation
of the initial phase. A plateau has been drawn somewhat arbitrarily
through the (111) data. Although the data scatter upwards from this
line, the clustering toward the bottom is sufficiently sharp to give
some credence to the plateau as drawn.

The behavior of the (100) data is different; it tends to drift
slowly upward in a manner which one might expect from a reaction
whose relaxation time is comparable to the time it takes a shock wave
to traverse the sample. The (111) plateau intersects both the linear
and quadratic fits to the B1 phase at $u_s$ = 5.94 and $u_p$ = 1.80 km/sec.
The pressure on the Hugoniot is 231 kb, the density is 3.105 $g/cm^3$
and the temperature is between 1120 and 1130 $^{O}K$. This number
should provide an upper bound to the actual transition pressure.

Basset, et. al.[11], have observed the B1-B2 transition at a
$V/V_0$ = 0.643 $\pm$ .002. Using our isotherm from the extrapolated
linear Hugoniot, we find the pressure of this transition as 307 $\pm$ 5kb.
The extrapolation of the quadratic fit would have yielded 295 $\pm$ 5 kb.
This should set the upper limit of pressure for the use of NaCl
in the B1 phase as an internal pressure standard at room temperature.

## Acknowledgements.

The authors would like to thank G. E. Hauver and A. Melani for the opportunity to look at their unpublished data and D. L. Decker for sending us his tabulated pressure-volume isotherms.

## References

1. J. C. Jamieson, Science 139, 1291 (1963).

2. D. L. Decker, J. Appl. Phys. 36, 157 (1965).

3. D. B. Larson, R. N. Keeler, A. Kusubov, and B. L. Hord, J. Phys. Chem. Solids 27, 476 (1966).

4. V. V. Evdokimova and L. F. Vereshchagin, J. Exp. Theor. Phys. 43, 1208 (1962); 16, 855 (1963).

5. C. W. F. T. Pistorius, J. Phys. Chem. Solids 25, 1477 (1964).

6. P. W. Bridgman, Proc. Am. Acad. Arts Sci. 76, 1 (1945).

7. Q. Johnson, Science 153, 419 (1966).

8. E. A. Perez-Albuerne and H. G. Drickamer, J. Chem. Phys. 43, 1381 (1965).

9. J. C. Jamieson, Physics of Solids at High Pressures, pp. 444-459, C. T. Tomizuka and R. M. Emrick, eds. (Academic Press, New York, 1965).

10. J. C. Jamieson, private communication.

11. W. A. Bassett, T. Takahashi, H. Mao, and J. S. Weaver, J. Appl. Phys. 39, 319 (1968).

12.  M. H. Rice, R. G. McQueen, and J. M. Walsh, Solid State
     Phys. $\underline{6}$, 1 (1958).

13.  W. J. Carter, S. P. Marsh, J. N. Fritz, and R. G. McQueen,
     "The Equation of State of Selected Materials for High Pressure
     References," NBS Symposium on the Accurate Characterization
     of the High Pressure Environment, Washington, 1968.

14.  S. Haussühl, Zeit. f. Physik $\underline{159}$, 223 (1960).

15.  R. A. Bartels and Schuele, D. E., J. Phys. Chem. Solids
     $\underline{26}$, 537 (1965).

16.  G. E. Hauver and A. Melani, private communication.

17.  W. H. Johnson, Jr. and A. O. Nier, Handbook of Physics,
     E. V. Condon and H. Odishaw, eds., pp. 9-65, 2nd ed.,
     (McGraw-Hill, New York, 1967).

18.  National Bureau of Standards Circular 539, $\underline{2}$, 41 (1965).

19.  T. Rubin, H. L. Johnston, and H. W. Altman, J. Chem. Phys.
     $\underline{65}$, 65 (1961).

20.  T. H. K. Barron, A. J. Leadbetter, and J. A. Morrison,
     Proc. Roy. Soc. A $\underline{279}$, 62 (1964).

21.  JANAF Thermochemical Tables, The Dow Chemical Company,
     Midland, Michigan.

22. R. Grover, R. N. Keeler, F. J. Rogers, and G. C. Kennedy, "On the Compressibility of the Alkali Metals," J. Phys. Chem. Solids (to be published).

23. R. N. Jeffery, J. D. Barnett, H. B. VanFleet, and H. T. Hall, J. Appl. Phys. 37, 3172 (1966).

24. D. B. McWhan, J. Appl. Phys. 38, 347 (1967).

## Table I. NaCl Hugoniot Data in the B1 Phase

| $u_s$ km/sec | $u_s$ std. km/sec | $u_p$ km/sec | P kb | $\rho$ g/cm$^3$ |
|---|---|---|---|---|
| (100 orientation) | | | | |
| 4.03 | 5.67 | 0.33 | 29 | 2.358 |
| 4.10 | 5.75 | 0.40 | 35 | 2.397 |
| 4.12 | 5.79 | 0.44 | 39 | 2.423 |
| 4.31 | 5.94 | 0.58 | 54 | 2.502 |
| 4.36 | 5.96 | 0.60 | 57 | 2.510 |
| 4.59 | 6.17 | 0.79 | 78 | 2.613 |
| 4.59 | 6.19 | 0.81 | 80 | 2.625 |
| 4.95 | 6.45 | 1.03 | 111 | 2.735 |
| 4.89 | 6.45 | 1.04 | 110 | 2.748 |
| 4.99 | 4.96* | 1.07 | 116 | 2.755 |
| 4.99 | 6.50 | 1.09 | 117 | 2.766 |
| 4.99 | 6.54 | 1.12 | 121 | 2.789 |
| 5.01 | 6.55 | 1.13 | 122 | 2.793 |
| 5.51 | 6.92 | 1.44 | 172 | 2.932 |
| 5.43 | 6.91 | 1.44 | 170 | 2.949 |
| 5.47 | 6.92 | 1.45 | 171 | 2.942 |
| (110) 5.47 | 6.92 | 1.45 | 171 | 2.941 |
| 5.59 | 5.41* | 1.53 | 184 | 2.977 |
| 5.67 | 7.07 | 1.57 | 193 | 2.992 |
| 5.84 | 5.58* | 1.70 | 215 | 3.052 |
| 5.94 | 7.36 | 1.82 | 234 | 3.121 |
| 5.96 | 7.37 | 1.84 | 237 | 3.129 |
| 6.12 | 7.47 | 1.92 | 254 | 3.151 |
| 6.12 | 7.47 | 1.92 | 254 | 3.152 |
| 6.15 | 7.51 | 1.95 | 259 | 3.166 |

Table I. - Page 2

| $u_s$ km/sec | $u_s$ std. km/sec | $u_p$ km/sec | P kb | $\rho$ g/cm$^3$ |
|---|---|---|---|---|
| 6.15 | 7.51 | 1.95 | 259 | 3.167 |
| 6.13 | 7.52 | 1.96 | 260 | 3.185 |
| 6.20 | 7.54 | 1.97 | 264 | 3.170 |

(1 1̄ 1 orientation)

| | | | | |
|---|---|---|---|---|
| 4.08 | 5.75 | 0.40 | 35 | 2.399 |
| 4.32 | 5.96 | 0.60 | 56 | 2.515 |
| 4.31 | 6.00 | 0.63 | 59 | 2.538 |
| 4.59 | 6.19 | 0.81 | 80 | 2.626 |
| 4.59 | 6.20 | 0.82 | 81 | 2.632 |
| 4.96 | 6.44 | 1.03 | 110 | 2.729 |
| 4.98 | 4.96* | 1.07 | 115 | 2.757 |
| 5.01 | 6.50 | 1.08 | 117 | 2.760 |
| 4.99 | 6.50 | 1.08 | 117 | 2.765 |
| 4.99 | 6.53 | 1.11 | 119 | 2.780 |
| 5.03 | 6.55 | 1.13 | 123 | 2.787 |
| 5.02 | 6.56 | 1.13 | 123 | 2.795 |
| 5.45 | 6.92 | 1.45 | 171 | 2.947 |
| 5.47 | 6.92 | 1.45 | 171 | 2.944 |
| 5.57 | 5.41* | 1.53 | 184 | 2.981 |

*Copper base plates. The rest are 2024 aluminum.

## Table II.  Thermodynamic Parameters for NaCl

| Quantity | Value | Reference |
|---|---|---|
| M | 58.443 g/mole | 17 |
| N | $6.02252 \times 10^{23}$ | |
| $a_0$ | 5.6393 Å at 22 °C | 19 |
| $\beta = \frac{1}{V}(\frac{\partial V}{\partial T})_P$ | $1.195 \times 10^{-4}/$°K at 20 °C | 19 |
| $B_s$ | 0.2505 Mb at 22 °C | 14 |
| $C_p$ | 12.05 cal/mole - °K at 20 °C | 20, 21 |

<u>Derived Values at 293 °K</u>

$\rho = 2.1645$ g/cm$^3$

$B_s = 0.2507$ Mb

$C_p = 0.8627 \times 10^6$ ergs/gm-°K

$c_0 = 3.403 \times 10^5$ cm/sec

$\gamma = \beta c_0^2/C_p = 1.6044$

$\gamma \beta T = 0.0562$

$C_V = 0.8168 \times 10^6$ ergs/gm-°K

$B_T = 0.2374$ Mb

$K_T = 4.213$ Mb$^{-1}$

$(\partial P/\partial T)_V = 0.0284$ Kb/°K

$(\partial E/\partial P)_V = 0.2880$ cm$^3$

$3nk = 0.8535 \times 10^7$ ergs/gm-°K

$C_V/3nk = 0.9570$

$\theta_D/T = 0.9420$

$\theta_D = 276$ °K

## Table III.   The $(\partial E / \partial P)_V$ Constant, 293 $^\circ$K  Na Cl Isotherm and its Antecedent Hugoniot

| | Hugoniot | | Isotherm | | |
|---|---|---|---|---|---|
| P | $\rho_H$ | $T_H$ | $\rho$ | $V/V_0$ | $a/a_0$ |
| Kb | g/cm$^3$ | $^\circ$K | g/cm$^3$ | | |
| 0 | 2.1645 | 293 | 2.1645 | 1.0000 | 1.0000 |
| 5 | 2.206 | 302 | 2.208 | .9803 | .9934 |
| 10 | 2.245 | 311 | 2.248 | .9629 | .9875 |
| 15 | 2.281 | 319 | 2.286 | .9469 | .9820 |
| 20 | 2.314 | 328 | 2.321 | .9326 | .9770 |
| 25 | 2.347 | 336 | 2.355 | .9191 | .9723 |
| 30 | 2.377 | 345 | 2.386 | .9072 | .9680 |
| 35 | 2.406 | 355 | 2.417 | .8955 | .9639 |
| 40 | 2.434 | 365 | 2.446 | .8849 | .9601 |
| 45 | 2.461 | 375 | 2.473 | .8753 | .9566 |
| 50 | 2.486 | 386 | 2.500 | .8658 | .9531 |
| 55 | 2.511 | 398 | 2.526 | .8569 | .9498 |
| 60 | 2.535 | 410 | 2.552 | .8482 | .9466 |
| 65 | 2.558 | 423 | 2.576 | .8403 | .9436 |
| 70 | 2.581 | 436 | 2.600 | .8325 | .9407 |
| 75 | 2.602 | 450 | 2.623 | .8252 | .9380 |
| 80 | 2.624 | 464 | 2.645 | .8183 | .9354 |
| 85 | 2.644 | 479 | 2.667 | .8116 | .9328 |
| 90 | 2.664 | 494 | 2.689 | .8049 | .9302 |
| 95 | 2.684 | 510 | 2.710 | .7987 | .9278 |
| 100 | 2.703 | 527 | 2.731 | .7926 | .9254 |
| 105 | 2.722 | 544 | 2.751 | .7868 | .9232 |
| 110 | 2.740 | 562 | 2.771 | .7811 | .9210 |
| 115 | 2.758 | 580 | 2.790 | .7758 | .9189 |

Table III. - Page 2

| P<br>Kb | $\rho_H$<br>g/cm$^3$ | $T_H$<br>$^{\circ}$K | $\rho$<br>g/cm$^3$ | $V/V_0$ | $a/a_0$ |
|---|---|---|---|---|---|
| 120 | 2.776 | 599 | 2.809 | .7706 | .9168 |
| 125 | 2.793 | 618 | 2.828 | .7654 | .9147 |
| 130 | 2.810 | 637 | 2.847 | .7603 | .9127 |
| 135 | 2.827 | 657 | 2.865 | .7555 | .9108 |
| 140 | 2.843 | 678 | 2.883 | .7508 | .9089 |
| 145 | 2.859 | 699 | 2.901 | .7461 | .9070 |
| 150 | 2.875 | 721 | 2.918 | .7418 | .9052 |
| 155 | 2.891 | 743 | 2.935 | .7375 | .9035 |
| 160 | 2.906 | 765 | 2.952 | .7332 | .9017 |
| 165 | 2.921 | 788 | 2.969 | .7290 | .9000 |
| 170 | 2.936 | 811 | 2.986 | .7249 | .8983 |
| 175 | 2.951 | 835 | 3.002 | .7210 | .8967 |
| 180 | 2.865 | 859 | 3.019 | .7170 | .8950 |
| 185 | 2.980 | 884 | 3.035 | .7132 | .8934 |
| 190 | 2.994 | 909 | 3.051 | .7094 | .8919 |
| 195 | 3.008 | 934 | 3.067 | .7057 | .8903 |
| 200 | 3.022 | 960 | 3.082 | .7023 | .8889 |
| 205 | 3.035 | 986 | 3.098 | .6987 | .8873 |
| 210 | 3.049 | 1013 | 3.113 | .6953 | .8859 |
| 215 | 3.062 | 1040 | 3.129 | .6918 | .8844 |
| 220 | 3.075 | 1067 | 3.144 | .6885 | .8830 |
| 225 | 3.089 | 1094 | 3.159 | .6852 | .8816 |
| 230 | 3.102 | 1123 | 3.174 | .6819 | .8802 |
| 235 | 3.114 | 1151 | 3.189 | .6787 | .8788 |
| 240 | 3.127 | 1180 | 3.204 | .6756 | .8774 |
| 245 | 3.140 | 1209 | 3.218 | .6726 | .8762 |
| 250 | 3.152 | 1238 | 3.233 | .6695 | .8748 |

Table III. - Page 3

| P Kb | $\rho_H$ g/cm$^3$ | $T_H$ $^o$K | $\rho$ g/cm$^3$ | $V/V_0$ | $a/a_0$ |
|---|---|---|---|---|---|
| 255 | 3.165 | 1268 | 3.247 | .6666 | .8736 |
| 260 | 3.177 | 1298 | 3.262 | .6635 | .8722 |
| 265 | 3.189 | 1328 | 3.276 | .6607 | .8710 |
| 270 | 3.201 | 1359 | 3.290 | .6579 | .8697 |
| 275 | 3.213 | 1390 | 3.304 | .6551 | .8685 |
| 280 | 3.225 | 1422 | 3.319 | .6522 | .8672 |
| 285 | 3.237 | 1453 | 3.333 | .6494 | .8660 |
| 290 | 3.249 | 1485 | 3.347 | .6467 | .8648 |
| 295 | 3.261 | 1518 | 3.360 | .6442 | .8637 |
| 300 | 3.272 | 1550 | 3.374 | .6415 | .8625 |
| 305 | 3.284 | 1583 | 3.388 | .6389 | .8613 |
| 310 | 3.295 | 1617 | 3.402 | .6362 | .8601 |
| 315 | 3.306 | 1650 | 3.415 | .6338 | .8590 |
| 320 | 3.318 | 1684 | 3.429 | .6312 | .8578 |

Table IV. The NaCl Isotherm above 200 kb using the Linear $u_s$-$u_p$ Fit

| | Hugoniot | | | Isotherm | | |
|---|---|---|---|---|---|---|
| P | $\rho_H$ | $T_H$ | | $\rho$ | $V/V_0$ | $a/a_0$ |
| Kb | g/cm$^3$ | $^{\circ}$K | | g/cm$^3$ | | |
| 200 | 3.023 | 950 | | 3.081 | .7025 | .8890 |
| 205 | 3.036 | 977 | | 3.096 | .6991 | .8875 |
| 210 | 3.050 | 1004 | | 3.111 | .6958 | .8861 |
| 215 | 3.063 | 1031 | | 3.126 | .6924 | .8847 |
| 220 | 3.075 | 1059 | | 3.140 | .6893 | .8834 |
| 225 | 3.088 | 1087 | | 3.154 | .6863 | .8821 |
| 230 | 3.100 | 1116 | | 3.168 | .6832 | .8808 |
| 235 | 3.113 | 1145 | | 3.182 | .6802 | .8795 |
| 240 | 3.125 | 1174 | | 3.196 | .6773 | .8782 |
| 245 | 3.137 | 1204 | | 3.210 | .6743 | .8769 |
| 250 | 3.148 | 1234 | | 3.223 | .6716 | .8757 |
| 255 | 3.160 | 1264 | | 3.236 | .6689 | .8745 |
| 260 | 3.171 | 1295 | | 3.249 | .6662 | .8734 |
| 265 | 3.183 | 1326 | | 3.262 | .6635 | .8722 |
| 270 | 3.194 | 1357 | | 3.275 | .6609 | .8711 |
| 275 | 3.205 | 1389 | | 3.288 | .6583 | .8699 |
| 280 | 3.216 | 1421 | | 3.300 | .6559 | .8689 |
| 285 | 3.227 | 1454 | | 3.313 | .6533 | .8677 |
| 290 | 3.238 | 1487 | | 3.325 | .6510 | .8667 |
| 295 | 3.248 | 1520 | | 3.337 | .6486 | .8656 |
| 300 | 3.259 | 1553 | | 3.349 | .6463 | .8646 |
| 305 | 3.269 | 1587 | | 3.361 | .6440 | .8636 |
| 310 | 3.279 | 1621 | | 3.373 | .6417 | .8625 |
| 315 | 3.289 | 1656 | | 3.384 | .6396 | .8616 |
| 320 | 3.299 | 1690 | | 3.396 | .6374 | .8606 |

Figure Captions

Fig. 1. The Shock Velocity-Particle Velocity Hugoniot of NaCl.
The elastic wave velocities were obtained from data in reference
(14). The larger symbols indicate multiple data points.

Fig. 2. The Various Functions Used for the Grüneisen Parameter.

Fig. 3. Pressure Variations in the Base Isotherm Due to Various
Changes in the Input Data. In this figure we show the fractional
change in pressure from the base isotherm,

$$\delta P/P = P \text{ (new parameters)}/P \text{ (base)} - 1,$$

at a given density. The actual abcissa is the pressure of the base
isotherm at this density.

Fig. 4. NaCl Isotherms. The solid line shows the isotherm
calculated from the quadratic fit to the Hugoniot in the $u_s - u_p$ plane.
The isotherm from the linear fit is parallel to Decker's isotherm and
roughly maintains a constant pressure offset from Decker's
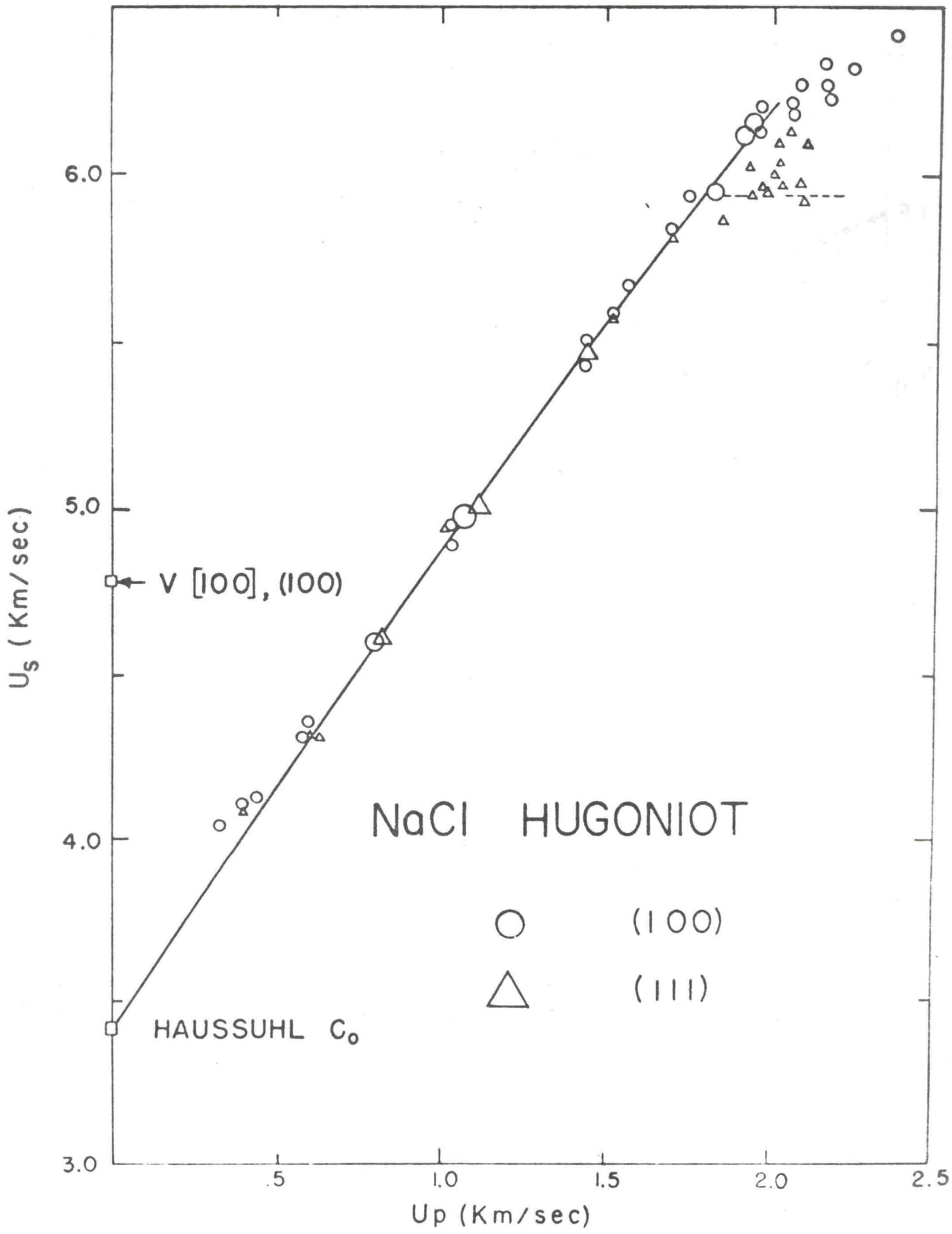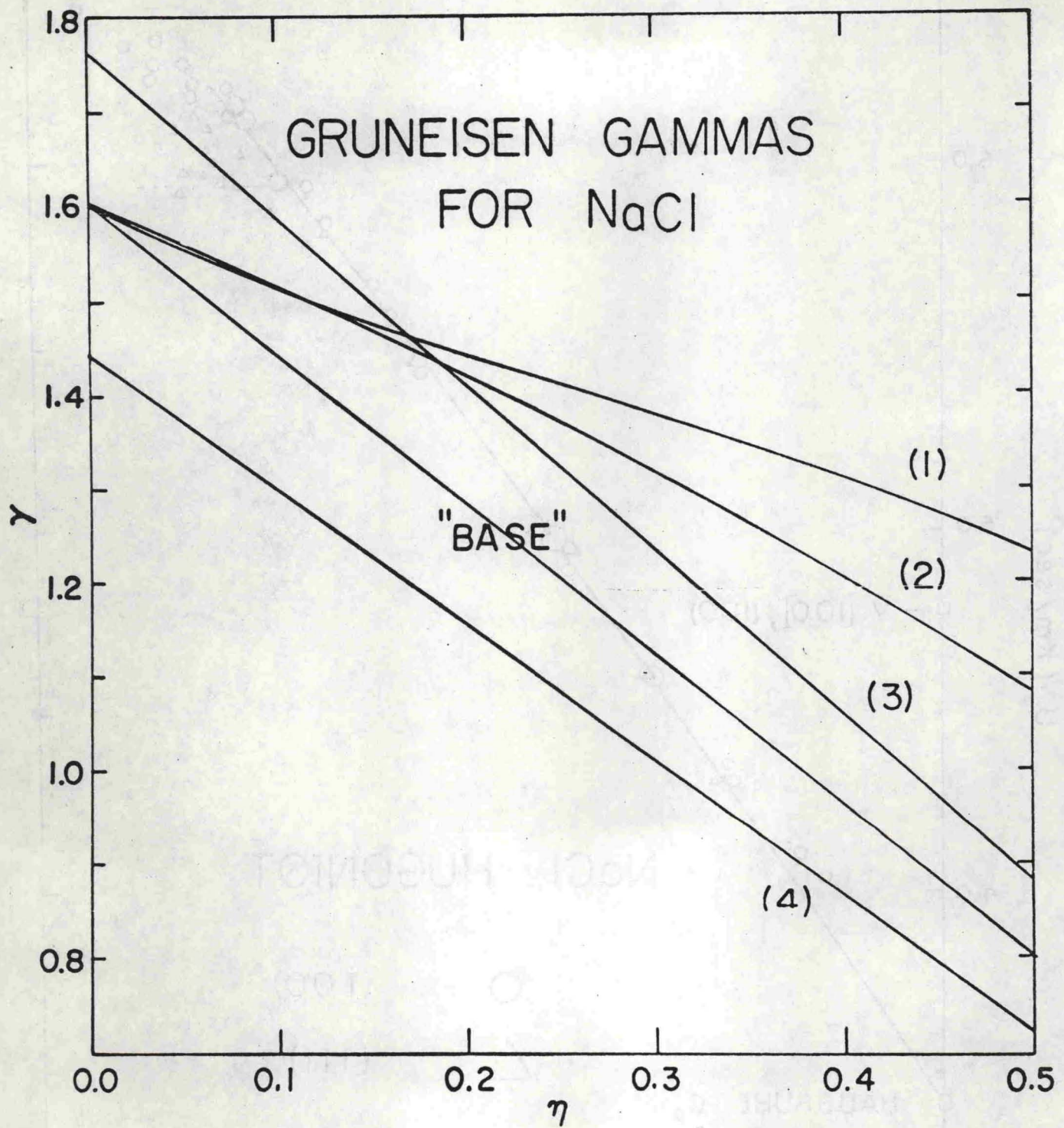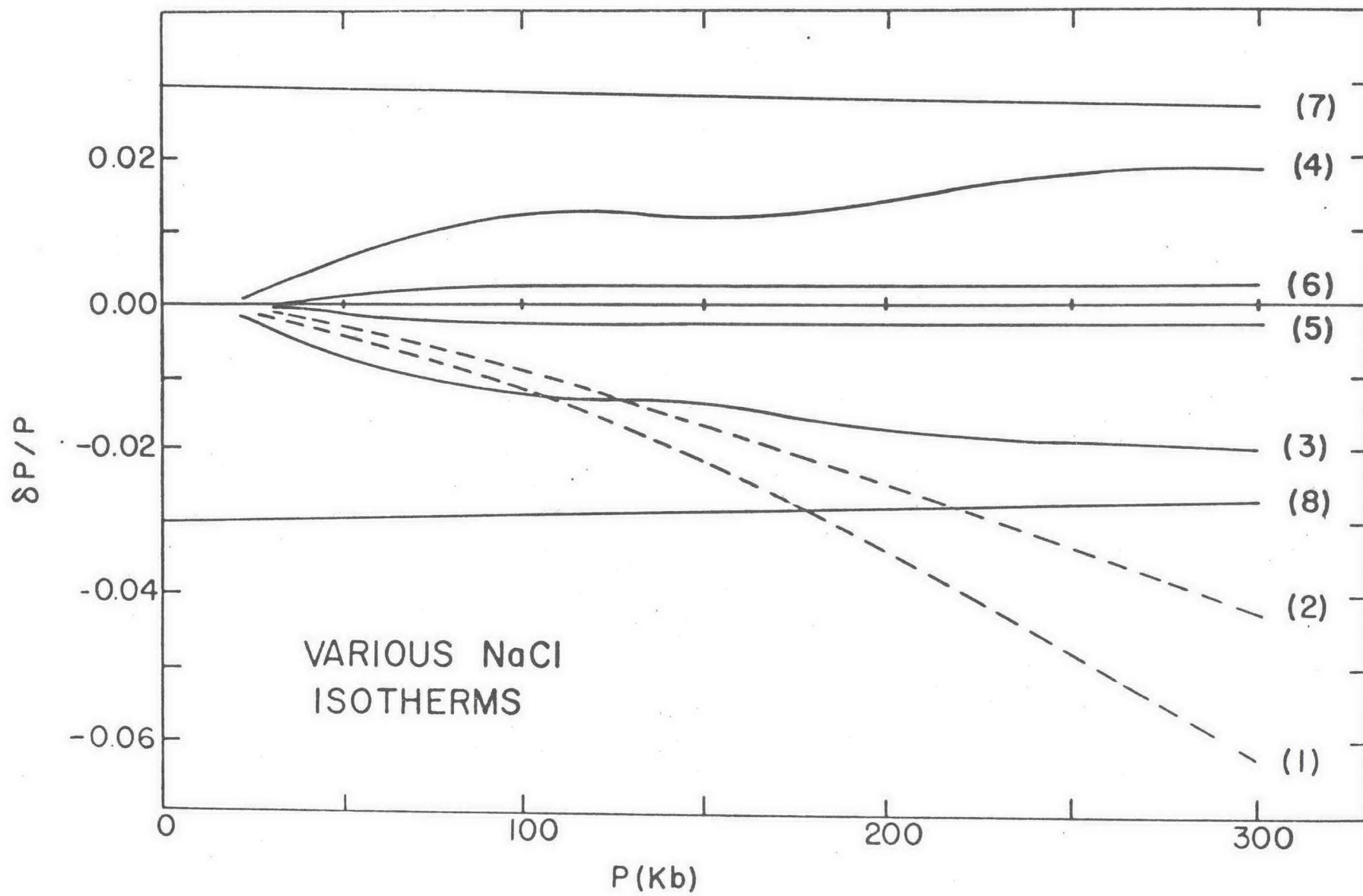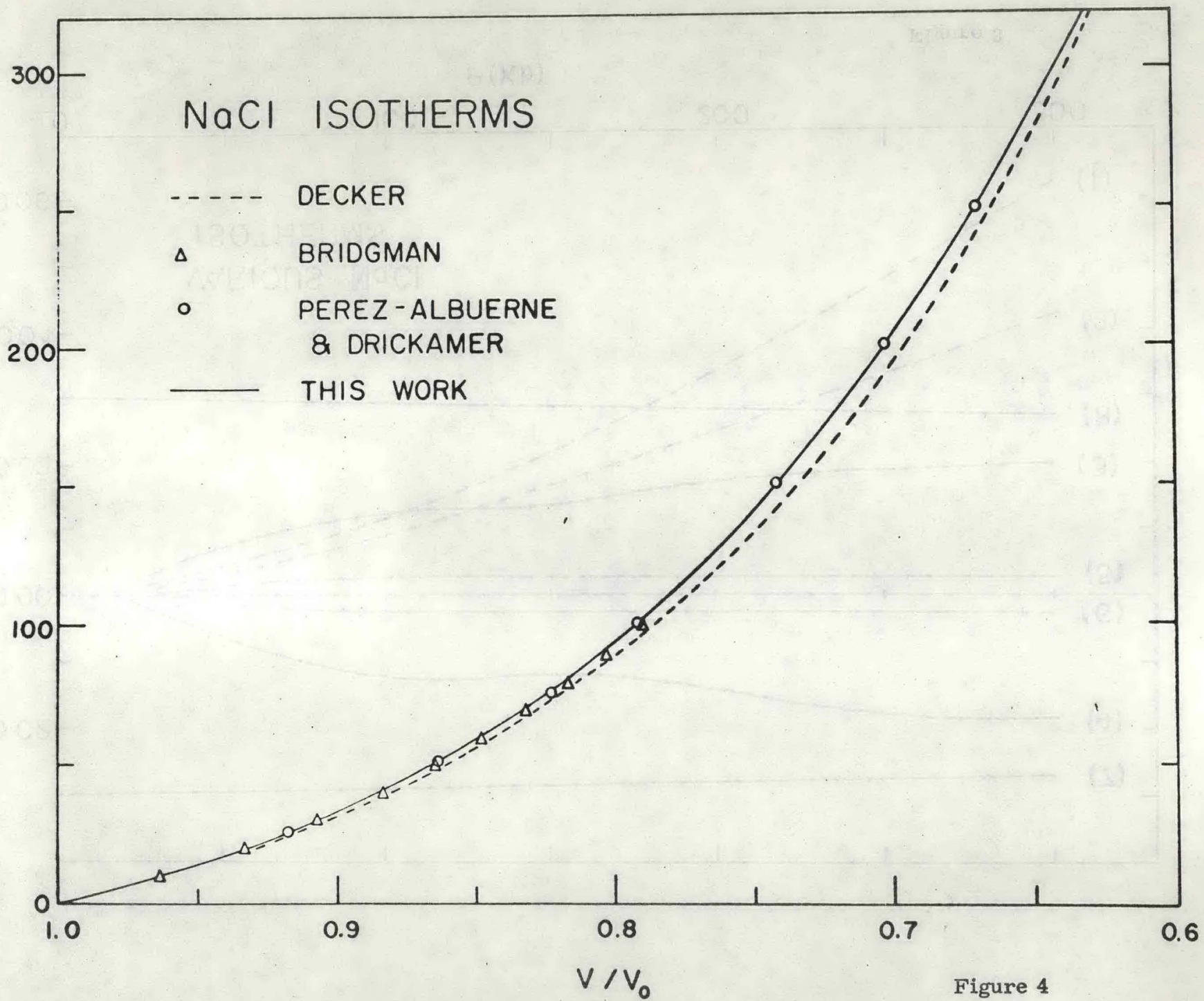isotherm from 200 to 320 kb.

Figure 1

Figure 2

Figure 3

NaCl ISOTHERMS

- - - - - DECKER
△ BRIDGMAN
○ PEREZ-ALBUERNE
  & DRICKAMER
——— THIS WORK

Figure 4